Supplemental Material

Supplemental Tables S1 - S2

Supplemental Figures S1 - S17

Table S1. Statistics of the hairpin-bisulfite sequencing data.

Sample	Bisulfite conversion rate	Total sequence (Gb)	Unique mapped Reads (Million)	Percentage of genome covered	Percentage of cytosine covered	Percentage of CpG covered	Average read depth for genome covered
E14-d0	98.9%	22.9	266.1	40.6	39.1	49.8	20.7
E14-d6	98.8%	25.7	273.8	34.0	32.1	41.6	27.7

Table S2. A summary of data sources on hairpin-bisulfite sequencing, RNA-seq, TAB-sequencing, and ChIP-seq for mouse embryonic stem cell line mES14TG2a.

GEO Accession	Data Type	Brief Description	Reference
GSE21442	ChIP-seq	H3K4me3	Illingworth et al., 2010
GSE11431	ChIP-seq	NANOG, OCT4, STAT3, SMAD1, SOX2, ZFX, MYC, MYCN, KLF4, ESRRB, TCFCP2l1, E2F1 , CTCF, p300 and SUZ12	Chen et al., 2008
GSE36114	ChIP-seq	H2AZ, H3K27ac, H3K27me3, H3K36me3, H3K4me1, H3K4me2 and H3K4me3	Xiao et al., 2012.
GSE24843	ChIP-seq	TET1	Kristine et al., 2011
GSE36173	TAB-seq	Hydroxymethylation	Yu et al., 2012
GSE48229	Hairpin-bisulfite sequencing	DNA methylation	This study
GSE48229	RNA-seq	Gene expression	This study

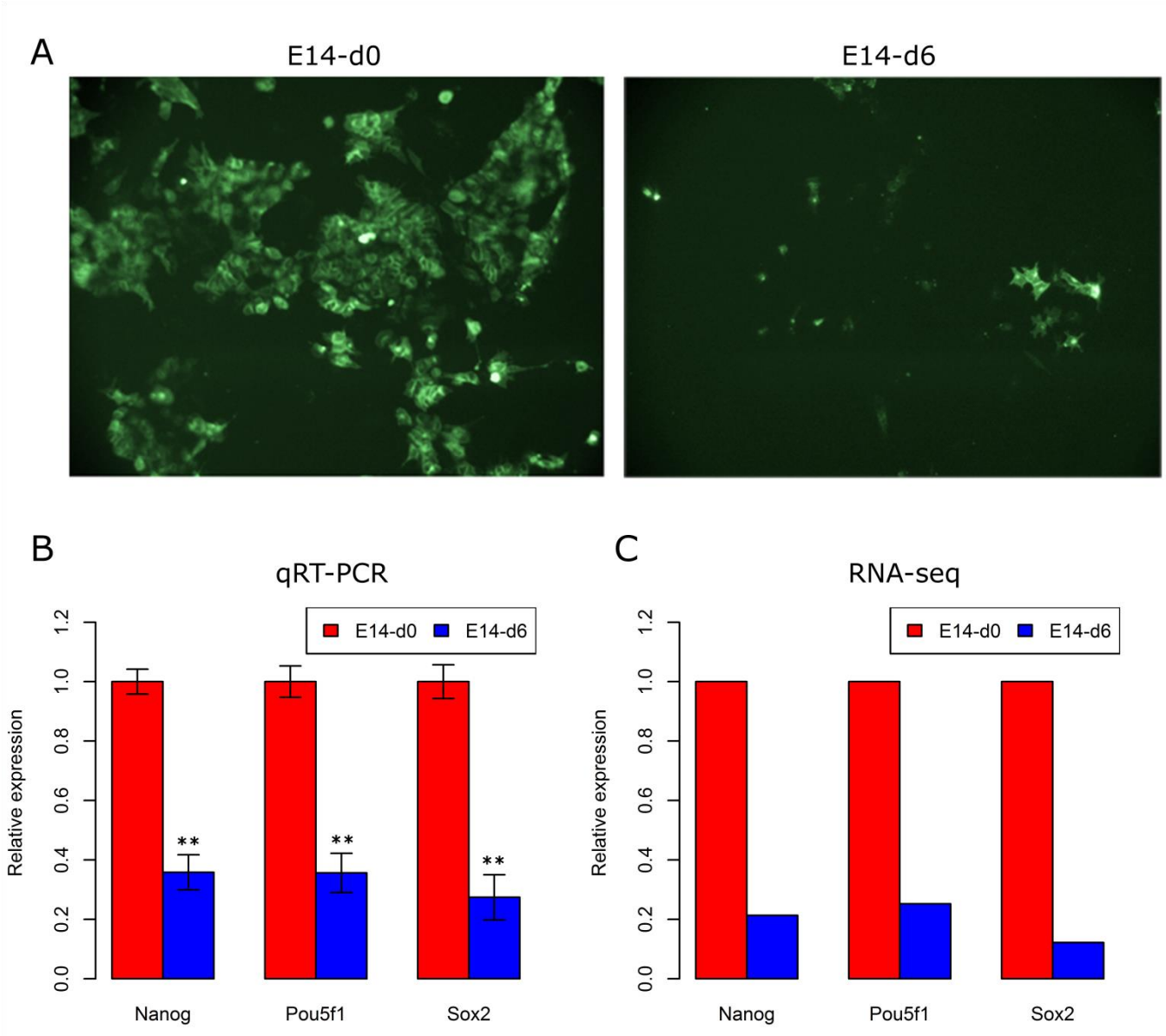

Figure S1. Comparison of the undifferentiated (E14-d0 cultured with LIF) and differentiating (E14-d6 cultured without LIF) states of mES cells. (A) Cells were stained with StainAlive™ SSEA-1 Antibody (DyLight™ 488). **(B)** Quantitative RT-PCR analysis of expression of *Nanog*, *Sox2*, and *Pou5f1* in undifferentiated and differentiating mES cells. Mean±SD values are shown. **, $p<0.01$; *t*-test. **(C)** RNA-seq expression analysis of *Nanog*, *Sox2*, and *Pou5f1* in undifferentiated and differentiating mES cells.

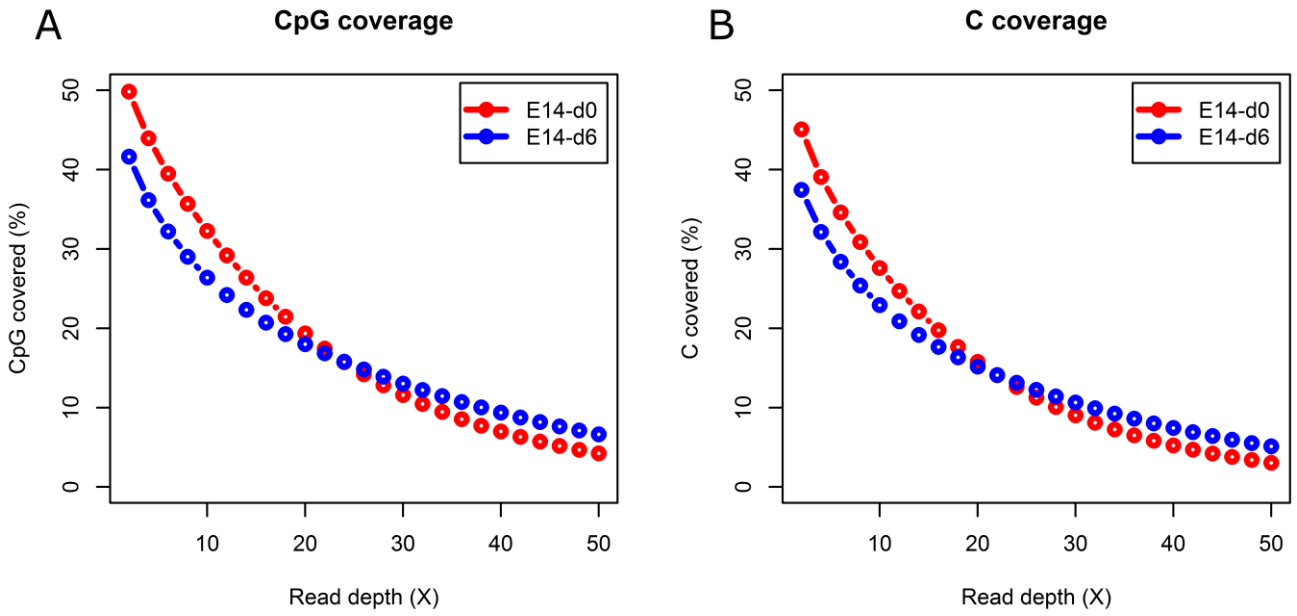

Figure S2. Percentages of covered CpGs and Cs at various sequencing depths.

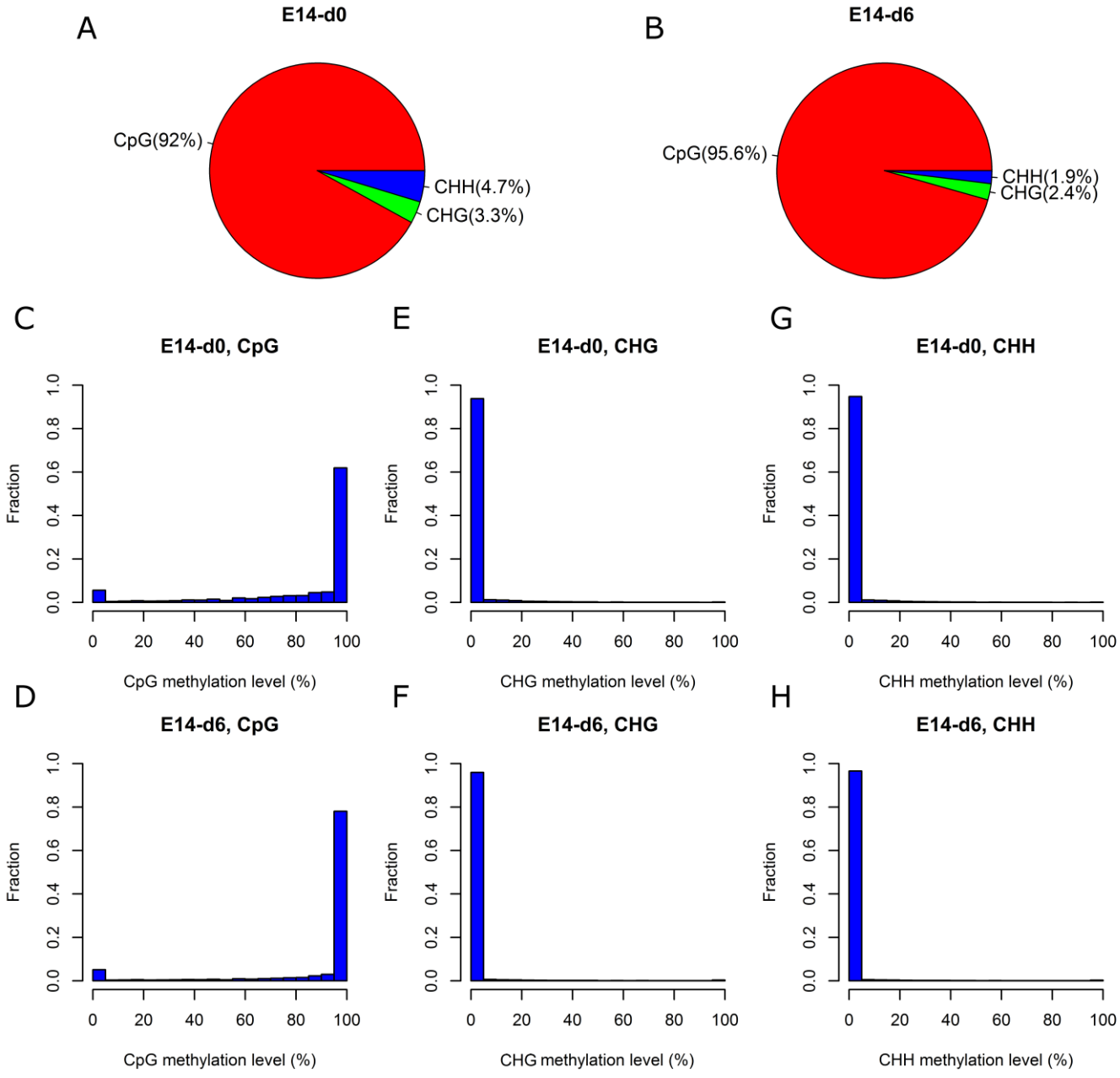

Figure S3. Global profiles of DNA methylation pattern. (A, B) Pie plots show the percentage of detected methyl-cytosines in CpG, CHG and CHH context for E14-d0 and E14-d6. **(C, D)** Distribution of methylation level of cytosines in CpG context. **(E, F)** Distribution of methylation level of cytosines in CHG context. **(G, H)** Distribution of methylation level of cytosines in CHH context.

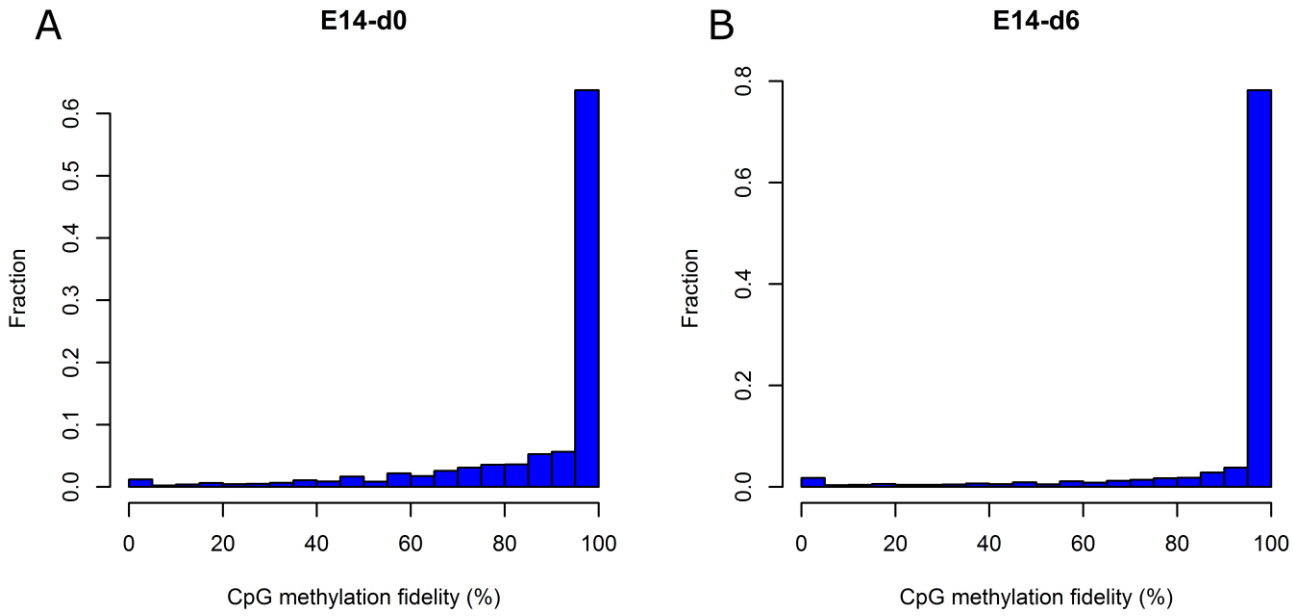

Figure S4. Distribution of CpG methylation fidelity. The histograms show the distribution of methylation fidelity in E14-d0 **(A)** and E14-d6 **(B)**, respectively.

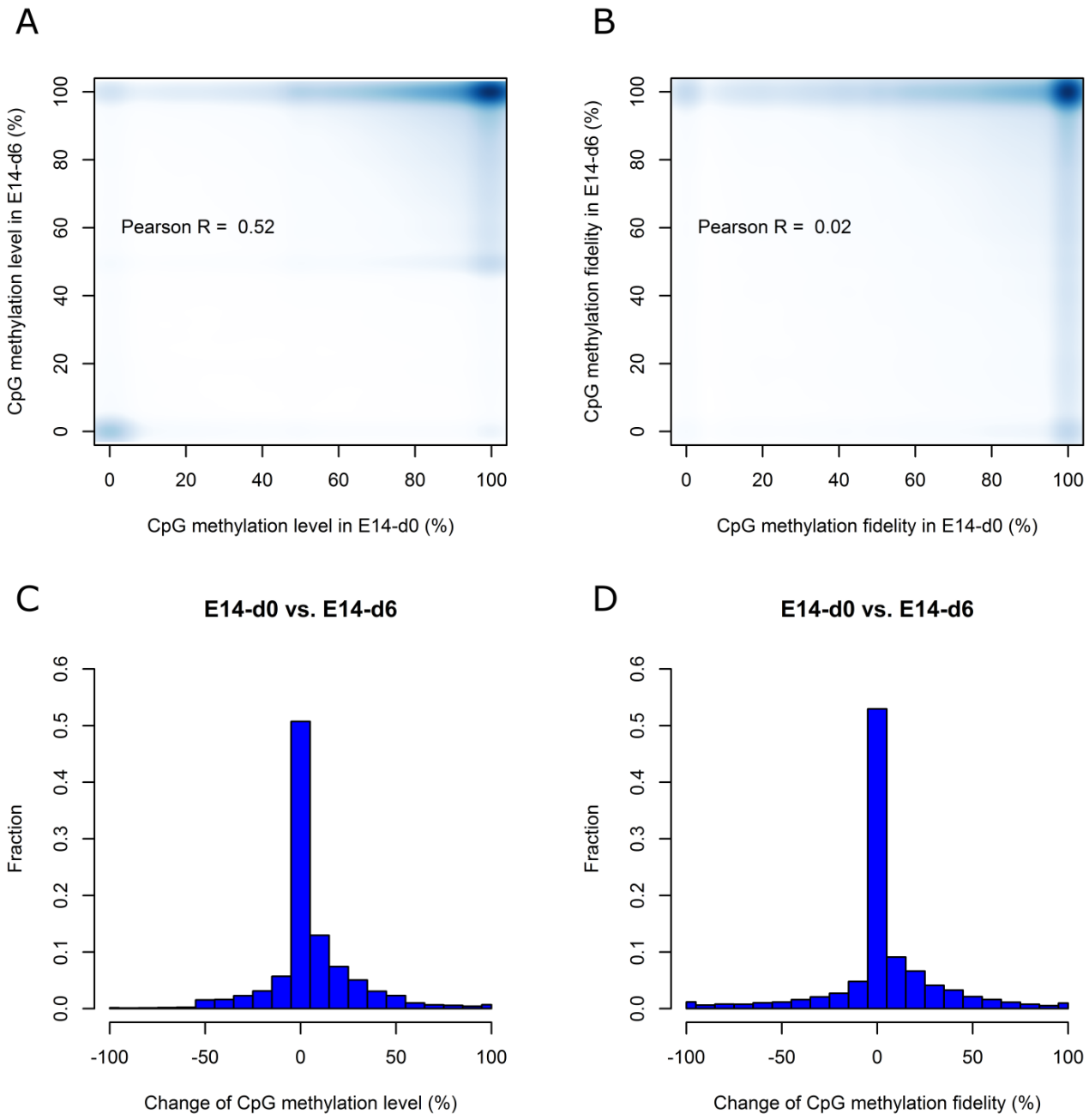

Figure S5. Changes of CpG methylation level and fidelity during mES cell differentiation. (A, B) Scatter plots showing the methylation level and methylation fidelity between E14-d0 and E14-d6. **(C, D)** The histograms showing the changes of methylation level and fidelity between E14-d0 and E14-d6. *x*-axis gives the changes of methylation level and fidelity of CpG sites in E14-d6 compared with those for E14-d0.

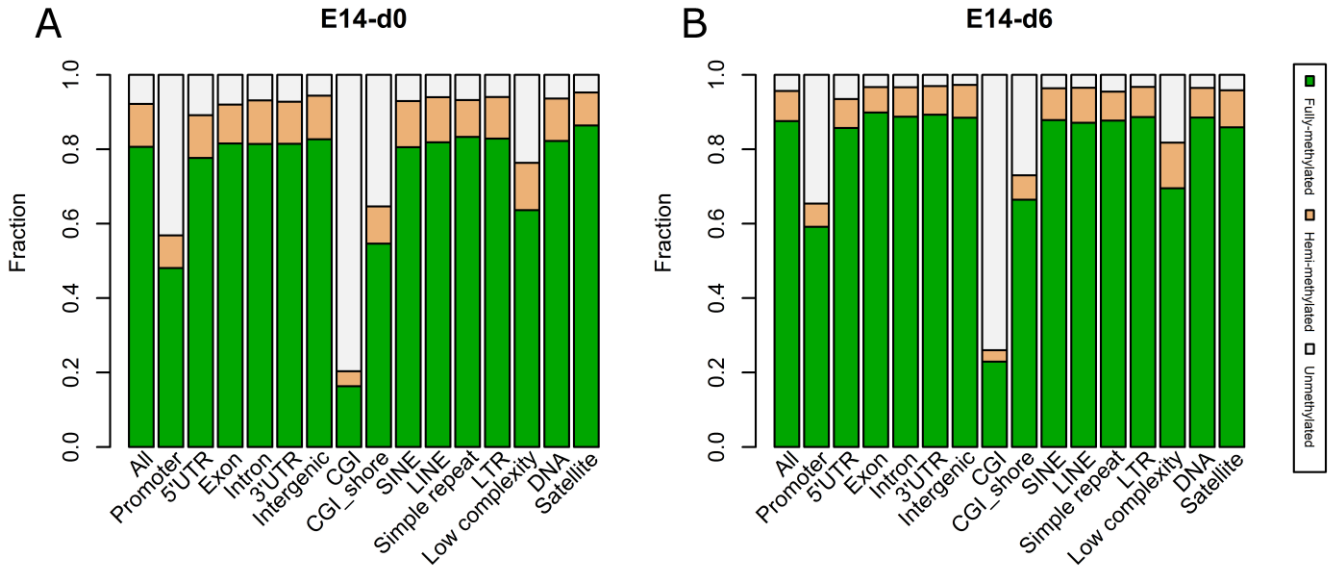

Figure S6. The proportion of unmethylated, hemi-methylated and fully methylated CpG dyads in different genomic regions. The bar plots show the proportions of unmethylated, hemi-methylated and fully methylated CpG dyads in E14-d0 **(A)** and E14-d6 **(B)**.

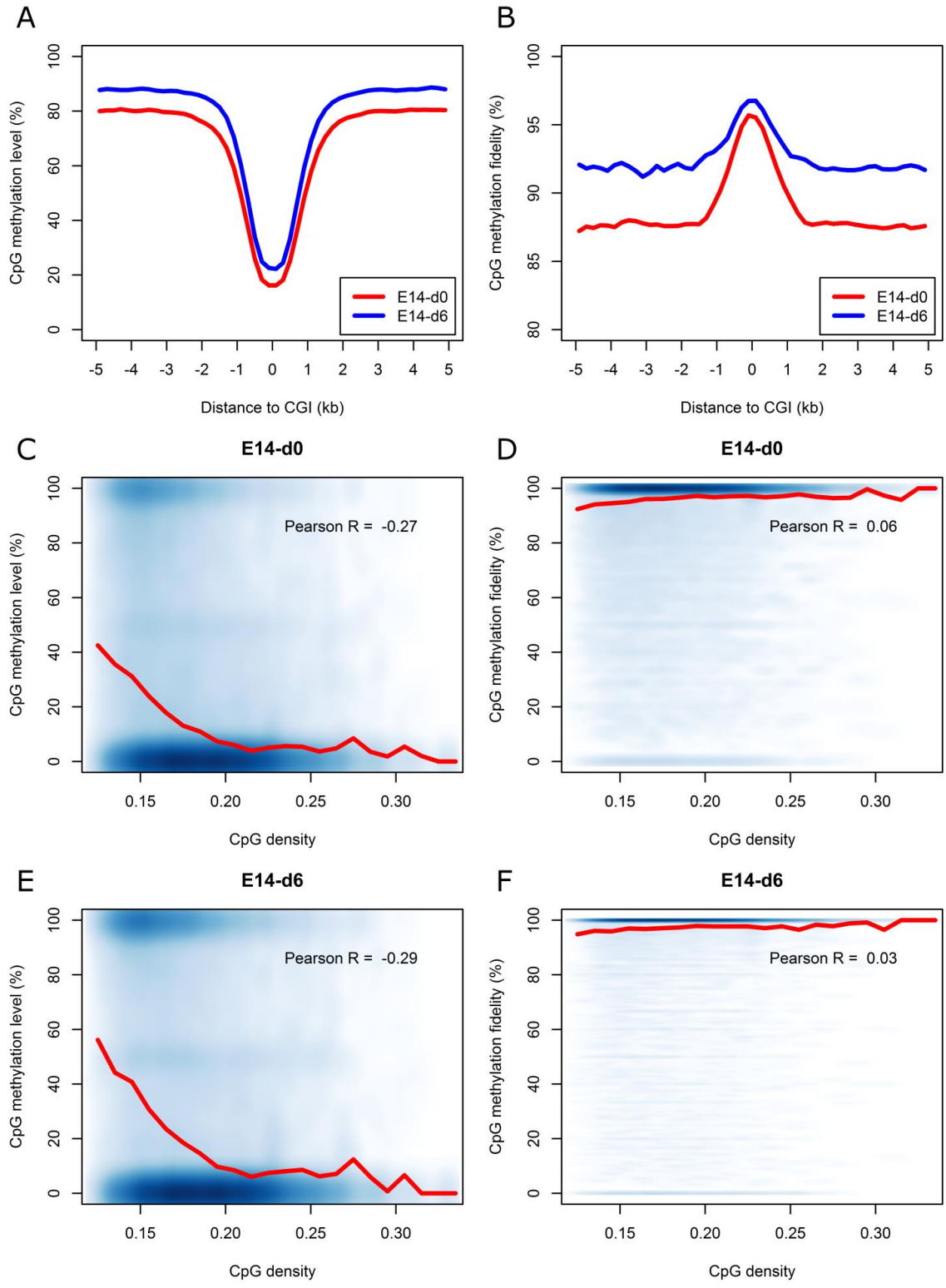

Figure S7. CpG methylation level and fidelity surrounding CpG islands. (A) Methylation level surrounding CGIs. **(B)** Methylation fidelity surrounding CGIs. The smoothed lines were calculated using 200-bp sliding windows. **(C, D)** Correlation between CpG density and CpG methylation level of CGIs. **(E, F)** Correlation between CpG density and CpG methylation fidelity of CGIs. The smoothed lines in C-F represent the mean values of CpG methylation levels along the changes of CpG density.

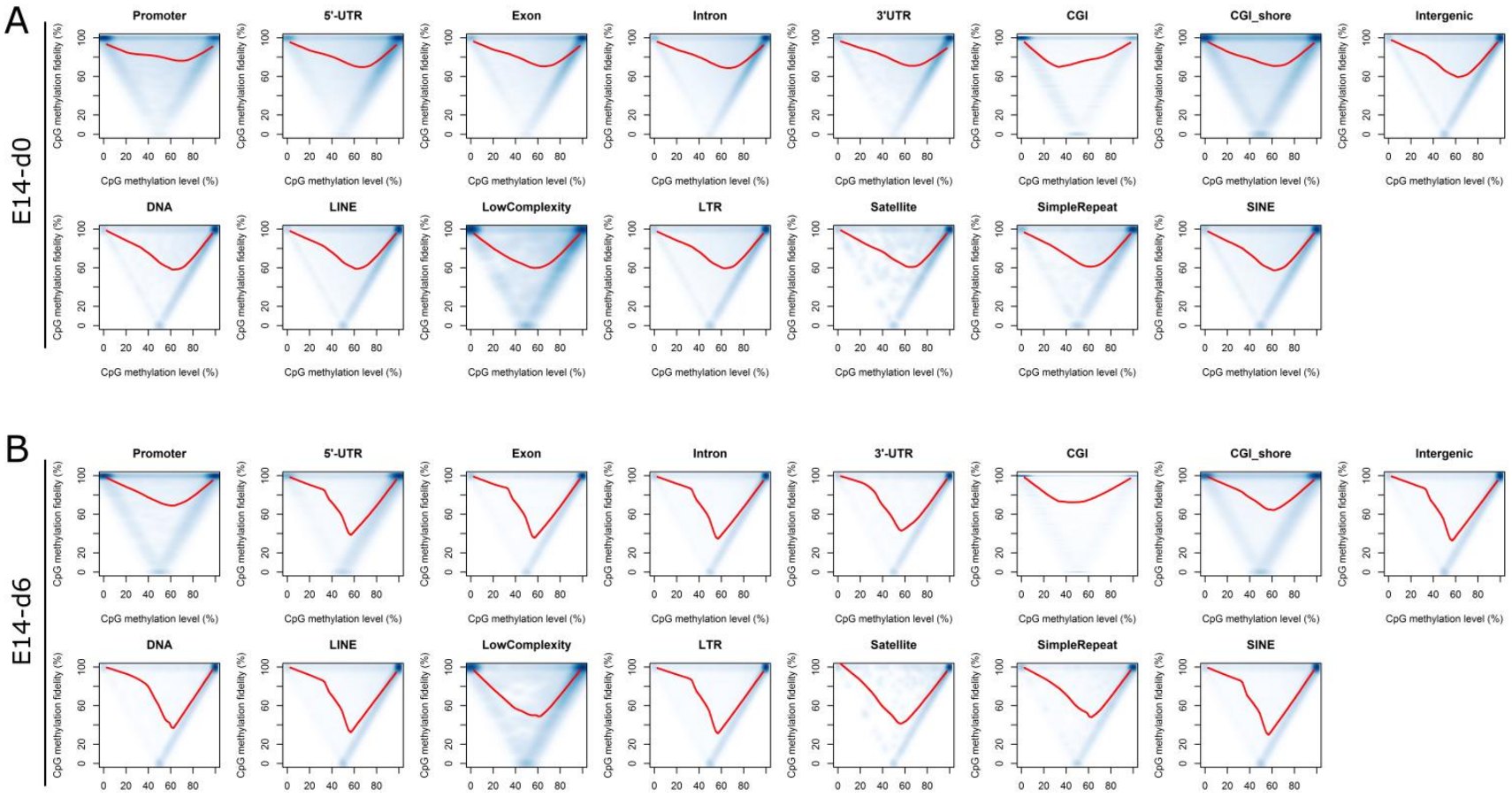

Figure S8. Relationships between CpG methylation level and fidelity in different genomic regions. The smoothed lines show the mean CpG methylation fidelity along with the change of methylation level.

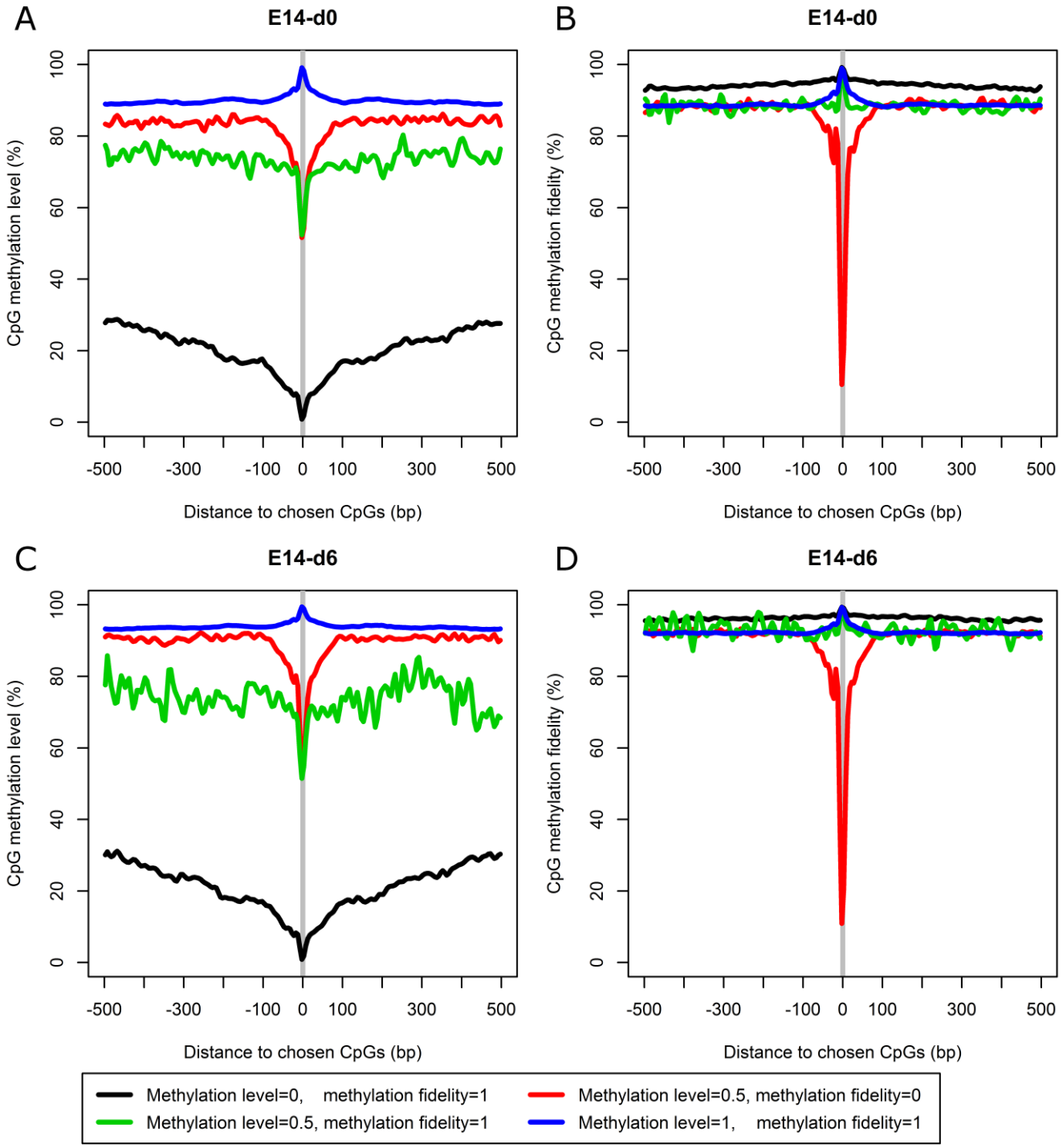

Figure S9. CpG methylation level and fidelity surrounding four groups of CpG dyads with ML=0&MF=1, ML=0.5&MF=0, ML=0.5&MF=1 and ML=1&MF=1. The smoothed lines show the profiles of CpG methylation level and fidelity surrounding each group of CpG dyads as calculated by using 5-bp sliding windows.

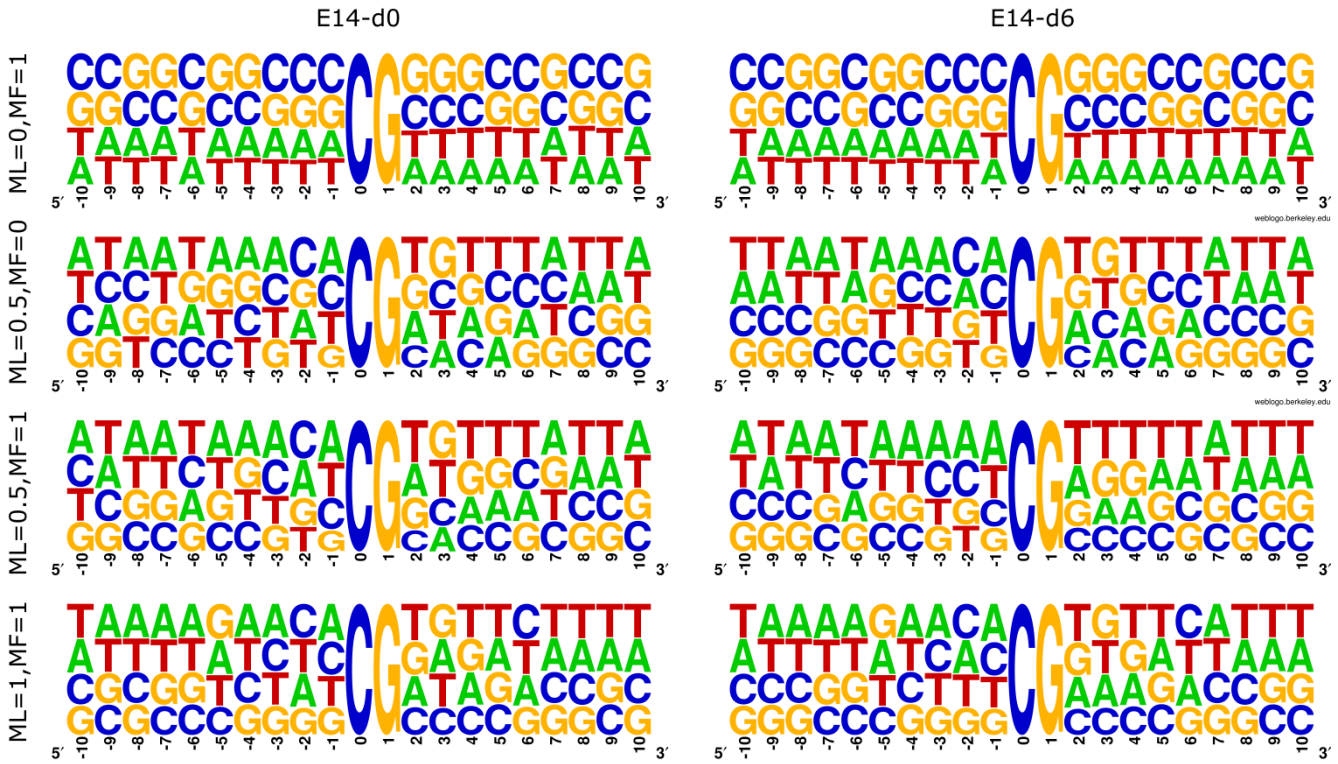

Figure S10. Residue preference surrounding the four groups of CpG dyads with ML=0&MF=1, ML=0.5&MF=0, ML=0.5&MF=1 and ML=1&MF=1.

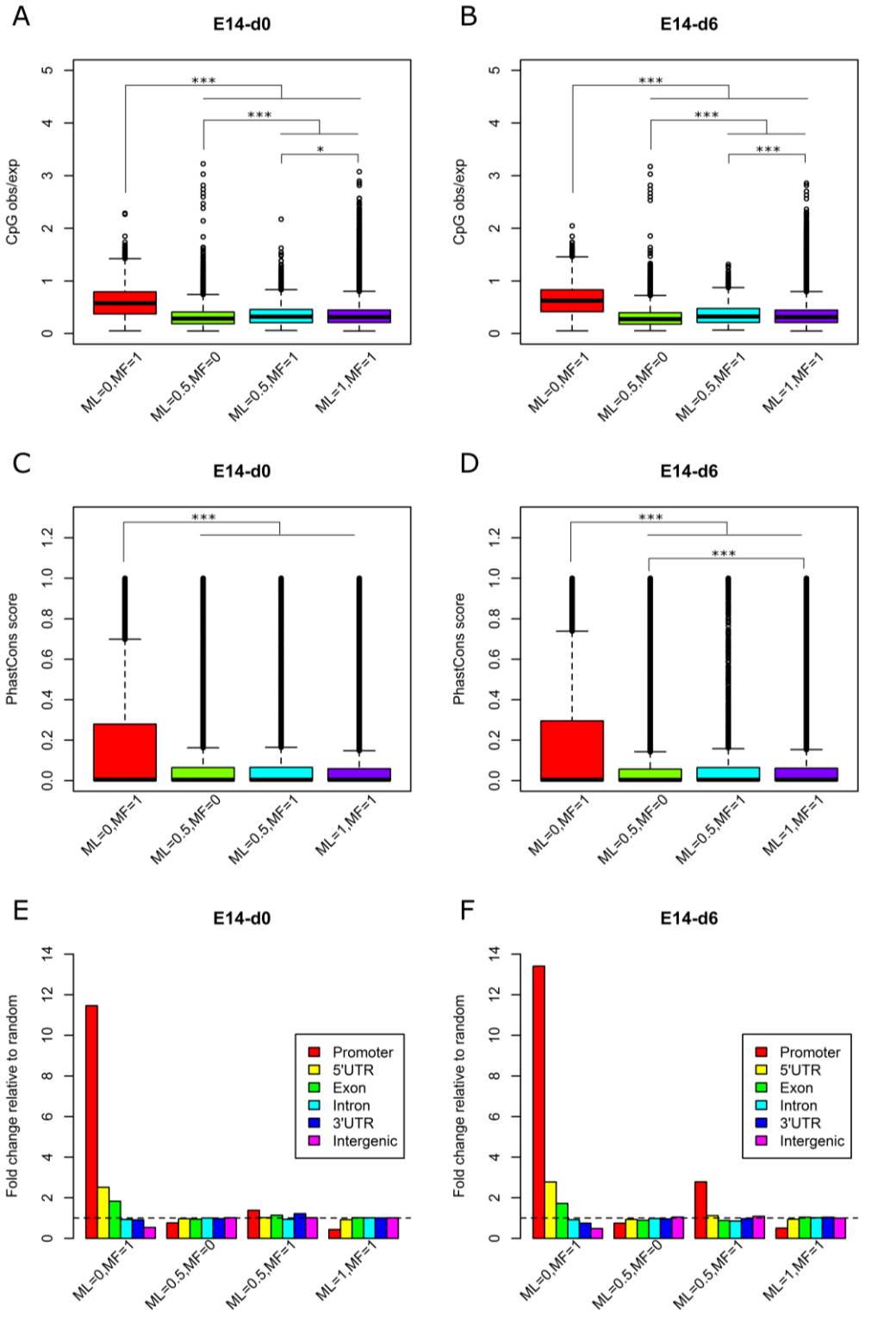

Figure S11. The comparison of CpG obs/exp, PhastCons score and genomic distribution among four groups of CpG dyads with ML=0&MF=1, ML=0.5&MF=0, ML=0.5&MF=1 and ML=1&MF=1. (A, B) CpG obs/exp for each CpG dyad is calculated based on 200-bp windows. Wilcoxon rank sum test were performed, with p-values indicated as * p<0.05, ** p<0.01, *** p<0.001. **(C, D)** The phastCons score for each groups CpG dyads. Wilcoxon rank sum test were performed, with p-values indicated as * p<0.05, ** p<0.01, *** p<0.001. **(E, F)** Fold change of genomic features associated with each groups of CpG dyads compared with random.

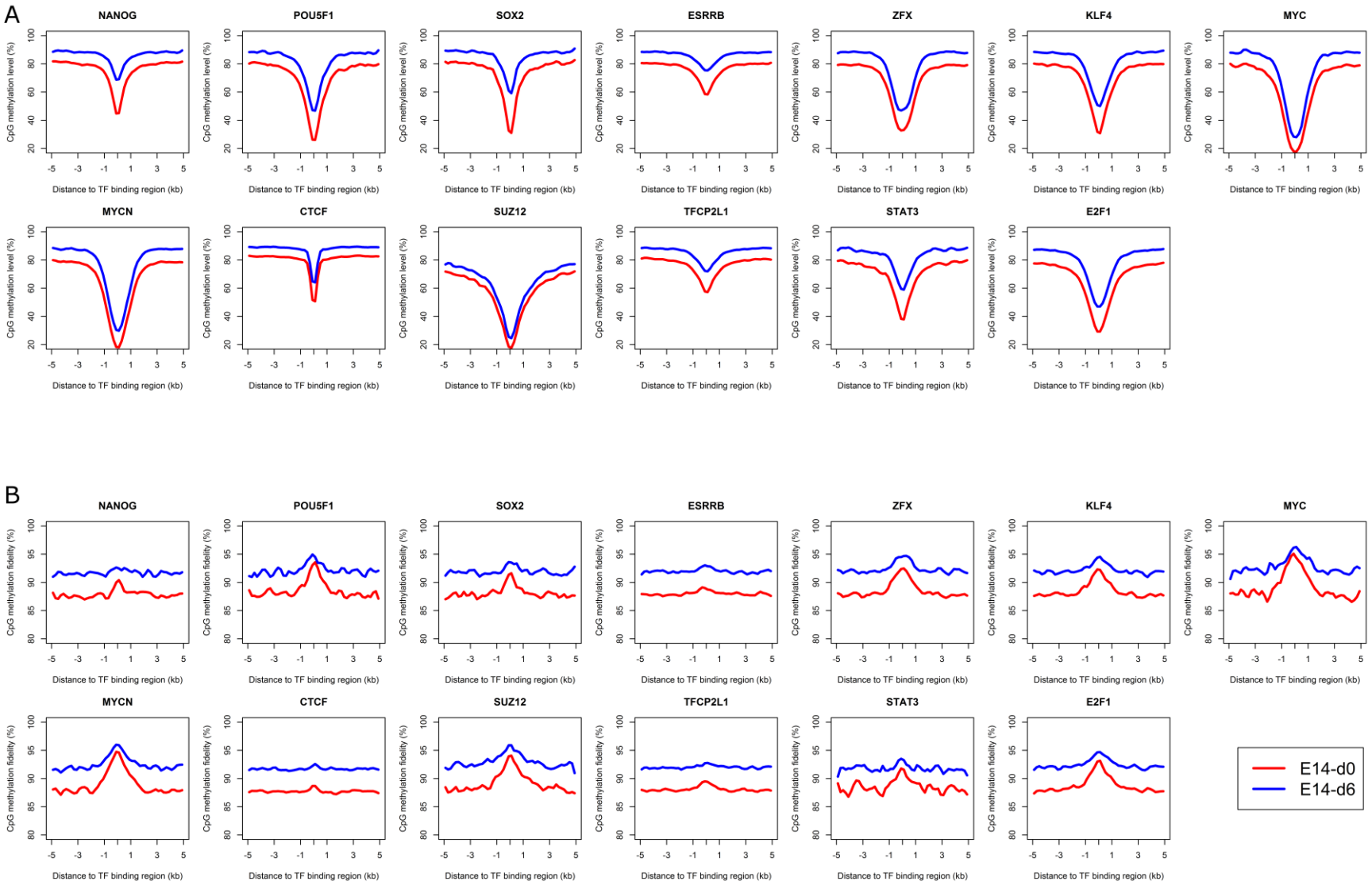

Figure S12. CpG methylation level and fidelity surrounding the ChIP-seq peaks for various transcription factors and regulators. The smoothed lines show the methylation level and fidelity surrounding TF binding regions as calculated using 200-bp sliding windows. The red lines show the result for E14-d0 and blue lines show that in E14-d6.

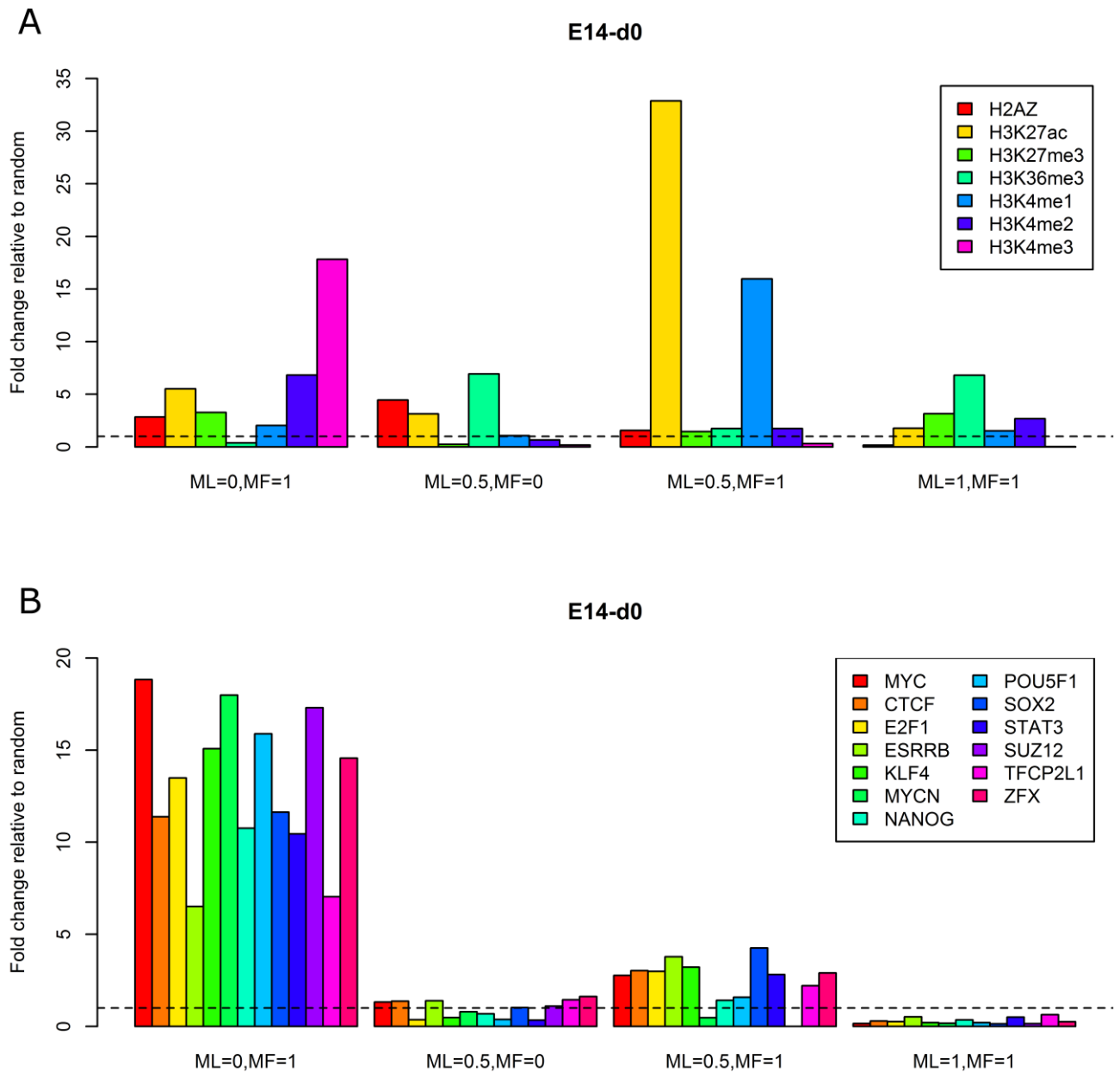

Figure S13. Co-occurrence of the four groups of CpG dyads with ML=0&MF=1, ML=0.5&MF=0, ML=0.5&MF=1 and ML=1&MF=1 at genomic loci with various histone modifications and TF bindings. The co-enrichments at genomic loci were demonstrated as fold change compared with random sets plotted as dashed lines.

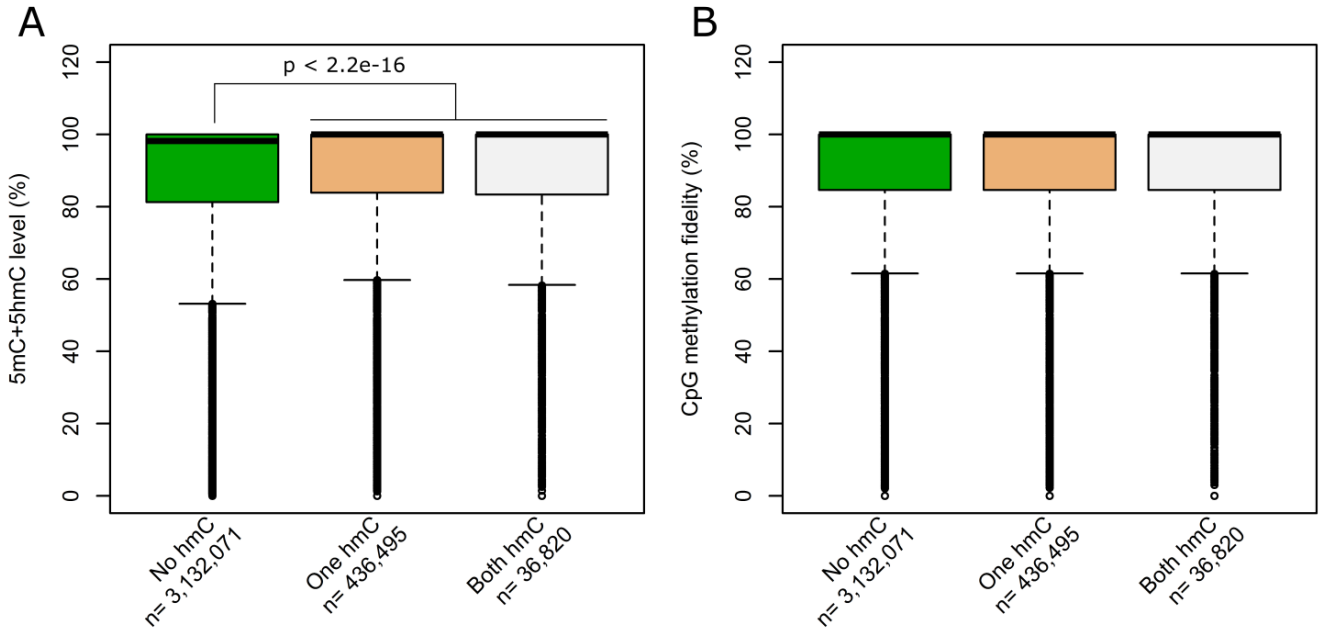

Figure S14. Relationship between DNA methylation and hydroxymethylation. Bar plots showing the methylation level **(A)** and fidelity **(B)** for CpG dyads with none, one, or both hydroxymethylated cytosines. The p-values for Wilcoxon rank sum test were indicated.

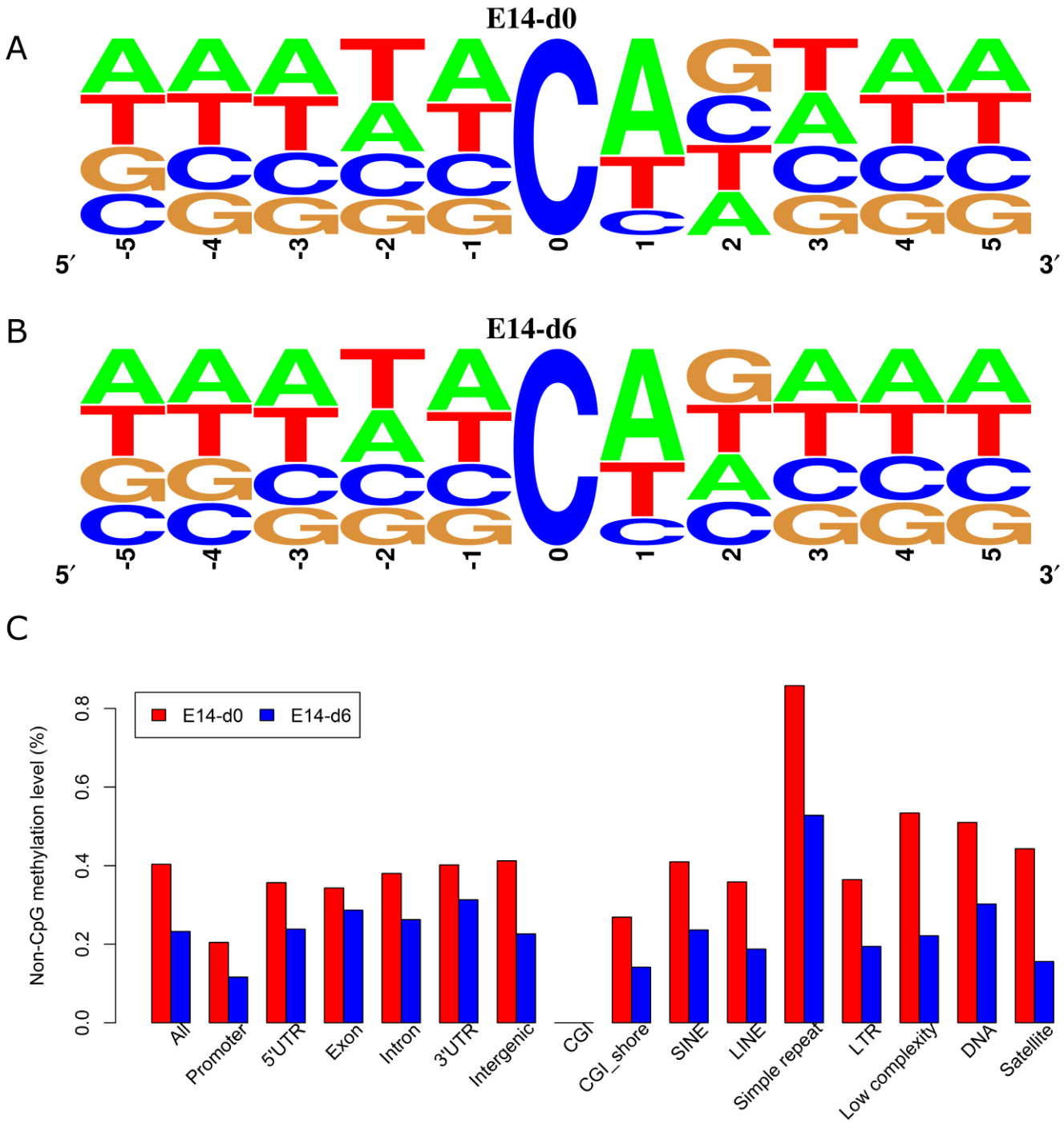

Figure S15. DNA methylation pattern of non-CpG sites. (A, B) weblogos show base frequencies surrounding methylated non-CpGs in E14-d0 **(A)** and E14-d6 **(B)**. **(C)** DNA methylation level of non-CpG sites in different genomic regions.

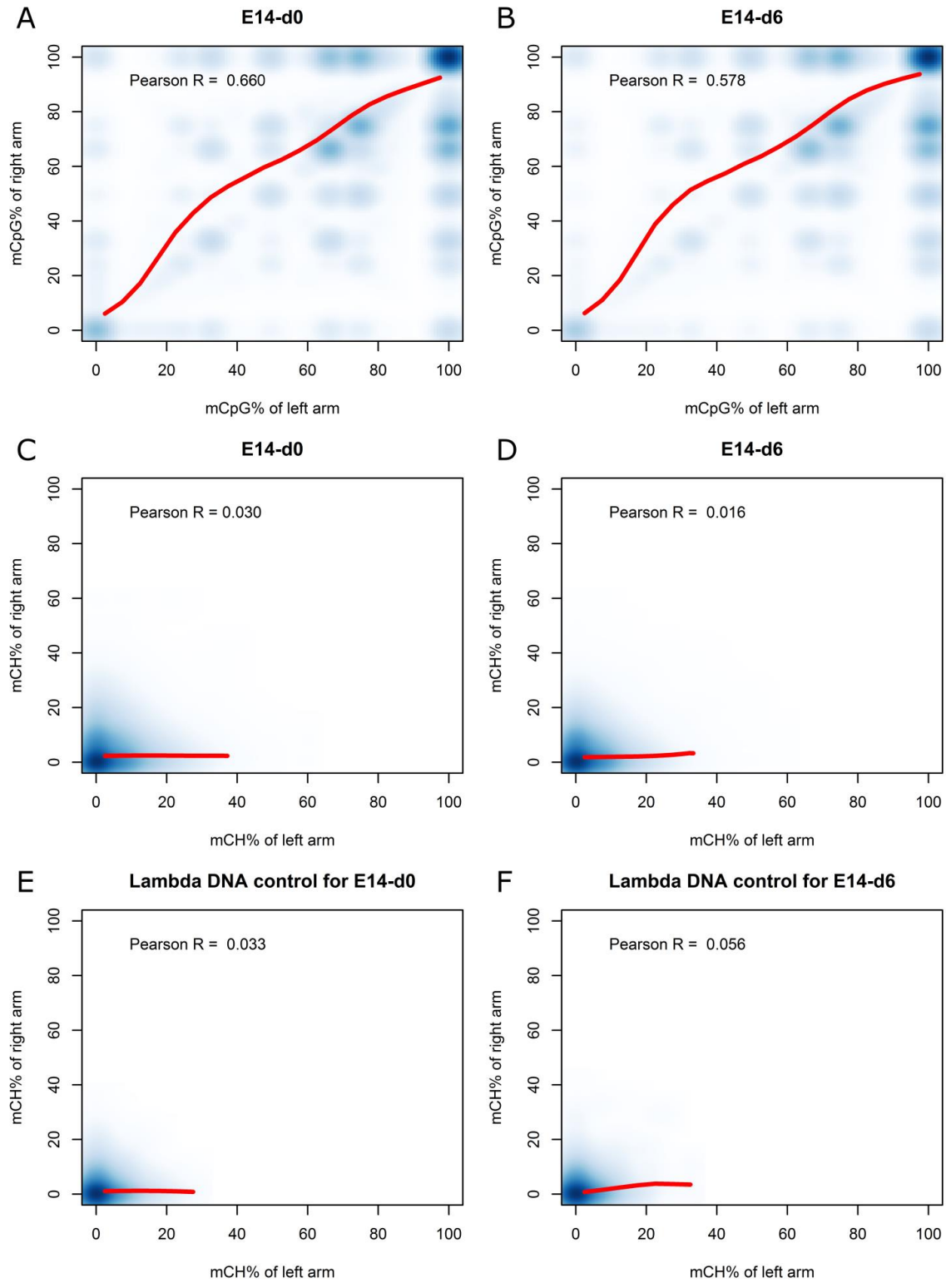

Figure S16. The correlation between the methylation levels of CpGs and non-CpGs in the two DNA complementary strands. (A, B) correlation between the methylation levels of CpG sites in the two DNA complementary strands for E14-d0 and E14-d6. **(C, D)** correlation between the methylation levels of Cs in non-CpG context in the two DNA complementary strands for E14-d0 and E14-d6. **(E, F)** correlation between the methylation levels of Cs in non-CpG context in the two DNA complementary strands of spike-in lambda control for E14-d0 and E14-d6. The smoothed lines represent the mean methylation levels determined in right arms along the change of those in left arms.

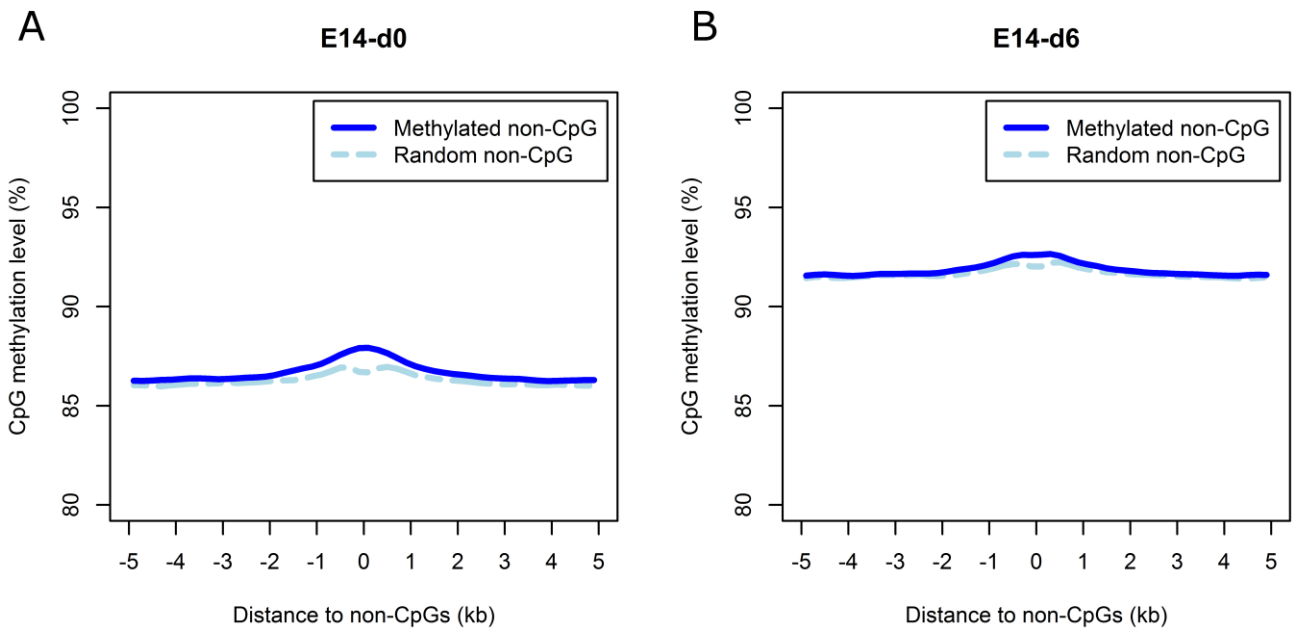

Figure S17. The association between non-CpG methylation and the methylation pattern of adjacent CpG dyads. (A, B) the methylation pattern of CpG dyads surrounding methylated Cs and random Cs in the non-CpG context in E14-d0 **(A)** and E14-d6 (B), respectively. The smoothed lines represent the CpG methylation level surrounding non-CpGs calculated using 200-bp sliding windows.